Since January 2020 Elsevier has created a COVID-19 resource centre with free information in English and Mandarin on the novel coronavirus COVID-19. The COVID-19 resource centre is hosted on Elsevier Connect, the company's public news and information website.

Available online at www.sciencedirect.com
ScienceDirect
Virology 368 (2007) 296–308
VIROLOGY
www.elsevier.com/locate/yviro

Absence of E protein arrests transmissible gastroenteritis coronavirus maturation in the secretory pathway

Javier Ortego [a,1], Juan E. Ceriani [b], Cristina Patiño [c], Juan Plana [b], Luis Enjuanes [a,*]

[a] *Centro Nacional de Biotecnología, CSIC, Department of Molecular and Cell Biology, Campus Universidad Autónoma, Darwin 3, Cantoblanco, 28049 Madrid, Spain*
[b] *Fort-Dodge Veterinaria, Department of Research and Development, Girona, Spain*
[c] *Centro Nacional de Biotecnología, CSIC, Macromolecular Structure, Campus Universidad Autónoma, Darwin 3, Cantoblanco, 28049 Madrid, Spain*

Received 12 March 2007; returned to author for revision 17 April 2007; accepted 14 May 2007
Available online 10 August 2007

Abstract

A recombinant transmissible gastroenteritis coronavirus (rTGEV) in which E gene was deleted (rTGEV-ΔE) has been engineered. This deletion mutant only grows in cells expressing E protein (E^+ cells) indicating that E was an essential gene for TGEV replication. Electron microscopy studies of rTGEV-ΔE infected BHK-pAPN-E^- cells showed that only immature intracellular virions were assembled. These virions were non-infectious and not secreted to the extracellular medium in BHK-pAPN-E^- cells. RNA and protein composition analysis by RNase-gold and immunoelectron microscopy showed that rTGEV-ΔE virions contained RNA and also all the structural TGEV proteins, except the deleted E protein. Nevertheless, full virion maturation was blocked. Studies of the rTGEV-ΔE subcellular localization by confocal and immunoelectron microscopy in infected E^- cells showed that in the absence of E protein virus trafficking was arrested in the intermediate compartment. Therefore, the absence of E protein in TGEV resulted in two actions, a blockade of virus trafficking in the membranes of the secretory pathway, and prevention of full virus maturation.

Keywords: Coronavirus; Nidovirus; E protein; TGEV; Virus maturation

Introduction

Since the identification of a novel coronavirus associated with severe acute respiratory syndrome (SARS), and the discovery of new human coronaviruses such as HCoV-NL63 and HCoV-NH, associated with respiratory illnesses, the interest on coronaviruses has clearly increased (Esper et al., 2005a, 2005b; Kuiken et al., 2003; van der Hoek et al., 2004). The design of antiviral drugs interfering with coronavirus replication (Hertzig et al., 2004) and the development of replication-competent propagation-deficient virus vectors (Ortego et al., 2002) are potential powerful tools to prevent and control coronavirus infections.

Transmissible gastroenteritis coronavirus (TGEV) is a member of the *Coronaviridae* family within the Nidovirales order (Enjuanes et al., 2000b). TGEV is an enveloped virus with a single-stranded, positive-sense RNA genome of 28.5 kb. About two-thirds of the genome encode the replicase gene, which comprises open reading frames 1a and 1b, the last one being expressed by ribosomal frameshifting (Brierley et al., 1989; Penzes et al., 2001). The 3′ one-third of the genome includes structural and nonstructural genes, in the order 5′-S-3a-3b-E-M-N-7-3′ (Enjuanes et al., 2000a).

In the *Coronaviridae* family, the viral envelope contains at least three structural proteins. The most abundant is the membrane (M) protein, spanning the membrane three or four times and interacting with the nucleocapsid (N) and spike (S) proteins during assembly (Escors et al., 2001; Rottier, 1995). The second most abundant is the S protein, a large type I-transmembrane glycoprotein that forms peplomers and is responsible for cell receptor binding and membrane fusion (Lewicki and Gallagher, 2002; Sui et al., 2004; Suñé et al., 1990; Suñé et al., 1991). The third is the small envelope (E) protein, a transmembrane protein detected as a minor structural component

* Corresponding author. Fax: +34 915854915.
E-mail address: L.Enjuanes@cnb.uam.es (L. Enjuanes).
[1] Present address: Centro de Investigación en Sanidad Animal, C.I.S.A.-I.N.I.A. Carretera Algete-El Casar, Km 8,100. Valdeolmos 28130. Madrid, Spain.

0042-6822/$ - see front matter © 2007 Elsevier Inc. All rights reserved.
doi:10.1016/j.virol.2007.05.032

in TGEV, mouse hepatitis virus (MHV), SARS-CoV, and avian infectious bronchitis virus (IBV) (Godet et al., 1992; Liu and Inglis, 1991; Shen et al., 2003; Yu et al., 1994). Another essential constituent of the virion is the N protein, an internal phosphoprotein that interacts with the genomic RNA to form the viral nucleocapsid (Escors et al., 2001; Kapke and Brian, 1986; Narayanan and Makino, 2001).

Coronavirus maturation takes place at the *cis*-Golgi network also known as endoplasmic reticulum-Golgi intermediate compartment (ERGIC) (Salanueva et al., 1999; Tooze et al., 1984, 1987). The E protein plays an important role during virus budding and transiently resides in a pre-Golgi compartment before progressing to the Golgi apparatus (Corse and Machamer, 2000; Maeda et al., 1999; Raamsman et al., 2000). It has been proposed that the E protein induces virus envelope curvature in pre-Golgi membranes during MHV and SARS-CoV infections (Arbely et al., 2004; Kuo et al., 2002). Studies on the assembly of coronavirus structural proteins by heterologous mammalian expression systems have shown that coexpression of E and M proteins from bovine coronavirus (BCoV), MHV, TGEV, IBV, and SARS-CoV results in the formation of virus like-particles (VLPs) that are morphologically identical to spikeless virions (Baudoux et al., 1998; Corse and Machamer, 2000; Hsieh et al., 2005; Kuo et al., 2007; Mortola and Roy, 2004; Vennema et al., 1996). In addition, it has been described that both the MHV and IBV E proteins are sufficient for the generation of VLPs (Corse and Machamer, 2000; Maeda et al., 1999). These observations suggested that neither the N nor the S proteins are needed for viral budding. In contrast, recent studies (Huang et al., 2004) described that M and N proteins are necessary and sufficient for the formation of SARS-CoV pseudoparticles. Therefore, the role of E protein in coronavirus morphogenesis requires additional studies.

The construction of coronavirus full length cDNA clones (Almazán et al., 2000; Casais et al., 2001; Thiel et al., 2001; Yount et al., 2000, 2003) or strategies of targeted recombination (Koetzner et al., 1992; Kuo et al., 2000; Masters, 1999) have allowed the manipulation of viral genomes to study coronavirus morphogenesis. Recently, a recombinant MHV virus with the entire gene E deleted was constructed (Kuo and Masters, 2003). This virus replicates with a low infectious titer, indicating that E protein is critical, but not essential for MHV replication in vitro. At variance, our laboratory has described an essential role for the E protein during TGEV replication. rTGEV-ΔE virus was rescued by complementation within E^+ packaging cell lines (Ortego et al., 2002).

In this article, we confirm that E protein is essential for TGEV replication in different cell lines, and report the first evidence that TGEV virions containing RNA are generated in absence of E protein, although virus maturation was arrested in the budding compartment, and immature virions were accumulated between the rough endoplasmic reticulum and *cis*-Golgi. These results provide evidence of an essential role of the E protein during TGEV morphogenesis and in the intracellular virus trafficking through the secretory pathway.

Results

Requirement of E protein for the generation of infective rTGEV-ΔE virus

A replication-competent propagation-deficient rTGEV-ΔE virus has been developed. This virus was rescued by complementation within E^+ packaging cell lines (Ortego et al., 2002). To determine whether TGEV propagation deficiency was dependent on the infected cell line, a collection of E^- cell lines permissive for TGEV replication (ST, CRFK, BHK-

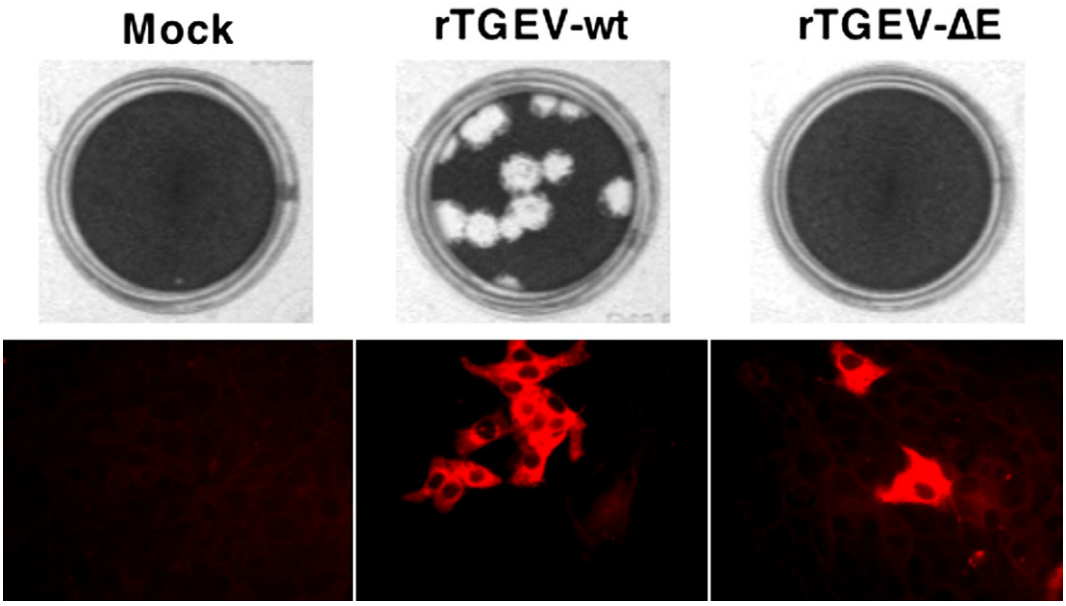

Fig. 1. Lack of rTGEV-ΔE propagation in E^- cell lines. Analysis of virus propagation in rTGEV-wt and rTGEV-ΔE infected ST-E^- cells at 24 and 96 h p.i., respectively, by plaque assay and immunofluorescence microscopy at 16 h p.i. using a TGEV specific serum. Mock, non-infected cells.

pAPN, and LLC-PK1) were infected with rTGEV-ΔE. Virus production was undetectable in infected BHK-pAPN, LLC-PK1, ST, and CRFK E^- cell lines either after 48 h post-infection or during four consecutive cell passages. In contrast, infection with rTGEV-ΔE of E^+ cell lines produced infective virus, with titers up to 10^7 pfu/ml in BHK-pAPN-E^+ and 10^6 pfu/ml in LLC-PK1-E^+. These data indicated that the lack of infectious rTGEV-ΔE virus production was independent of the cell line.

To confirm the propagation deficiency of rTGEV-ΔE, ST-E^- cells were infected with this virus and the propagation analyzed by plaque assay and immunofluorescence microscopy. Lysis plaques were observed in monolayers of ST-E^- cells infected with rTGEV-wt at 24 h post-infection, whereas no plaques were generated by rTGEV-ΔE in these cells up to 96 h post-infection (Fig. 1). Immunofluorescence microscopy of ST-E^- cells infected at low m.o.i. (0.05) showed groups of cells infected by rTGEV-wt at 16 h post-infection. In contrast, single infected ST-E^- cells were observed in monolayers infected with rTGEV-ΔE virus (Fig. 1) at the same time post-infection and, later in the infection, the cells died and the fluorescence disappear (data not shown), suggesting that ΔE virions did not spread to neighboring uninfected cells and confirming that rTGEV-ΔE was a replication-competent propagation-deficient virus.

Formation of TGEV virions in the absence of E protein

BHK-pAPN-E^+ and E^- cells infected with rTGEV-ΔE virus were analyzed by electron microscopy to determine the formation of TGEV virions. Mature forms of the virions showing a dense core (60-nm diameter), preferentially located inside secretory vesicles, were abundant in infected BHK-pAPN-E^+ cells at 24 h post-infection (Figs. 2A, E^+), whereas large virus-like particles, exhibiting an electron dense periphery and a translucent central zone, were unexpectedly observed in infected BHK-pAPN-E^- cells at the same time post-infection (Figs. 2A, E^-). These large virus-like particles resembled the TGEV immature virions previously reported (Risco et al., 1998) but with a higher diameter (larger than 80-nm). Mature intracellular

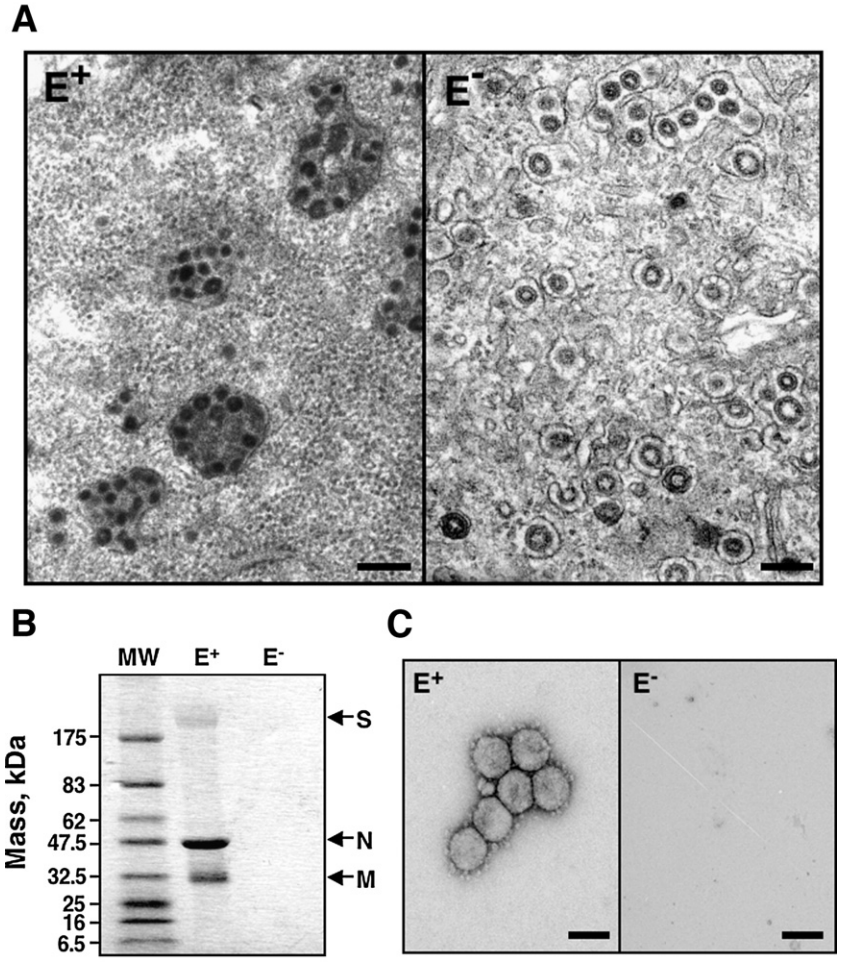

Fig. 2. Characterization of intracellular and extracellular rTGEV-ΔE virus in BHK-pAPN-E^+ and E^- cells. (A) Assembly characterization of rTGEV-ΔE in BHK-pAPN-E^+ and E^- cells by electron microscopy. Panels show sections from rTGEV-ΔE infected BHK-pAPN-E^+ and E^- cells at 24 h p.i. Scale bars, 300 nm. (B) The presence of TGEV proteins in supernatants was analyzed by SDS-PAGE using 5 to 20% gradient gels and silver staining. The arrows to the right of the panel indicate the positions of TGEV structural proteins. (C) Electron micrographs of virions from supernatants of rTGEV-ΔE infected BHK-pAPN-E^+ and E^- cells concentrated 200-fold, and stained with 2% uranyl acetate are shown. Scale bar, 100 nm.

virions were not observed in rTGEV-ΔE infected BHK-pAPN-E$^-$ cells.

To determine whether mature or immature virions were secreted from rTGEV-ΔE infected BHK-pAPN-E$^-$ cells, the presence of virions in the supernatants of infected BHK-pAPN-E$^+$ and E$^-$ cells was analyzed after virion purification by silver-staining SDS-PAGE and negative-staining electron microscopy (Fig. 2). No structural TGEV proteins were detected in the supernatants of BHK-pAPN-E$^-$ cells infected with rTGEV-ΔE at 48 h post-infection, whereas S, M, and N proteins were detected in the supernatants of infected cells expressing E protein (Fig. 2B). The absence of secreted virions in BHK-pAPN-E$^-$ cells infected with rTGEV-ΔE was confirmed by negative-staining electron microscopy on 200-fold concentrated supernatants, whereas virions were observed in supernatants of BHK-pAPN-E$^+$ infected cells (Fig. 2C). These observations

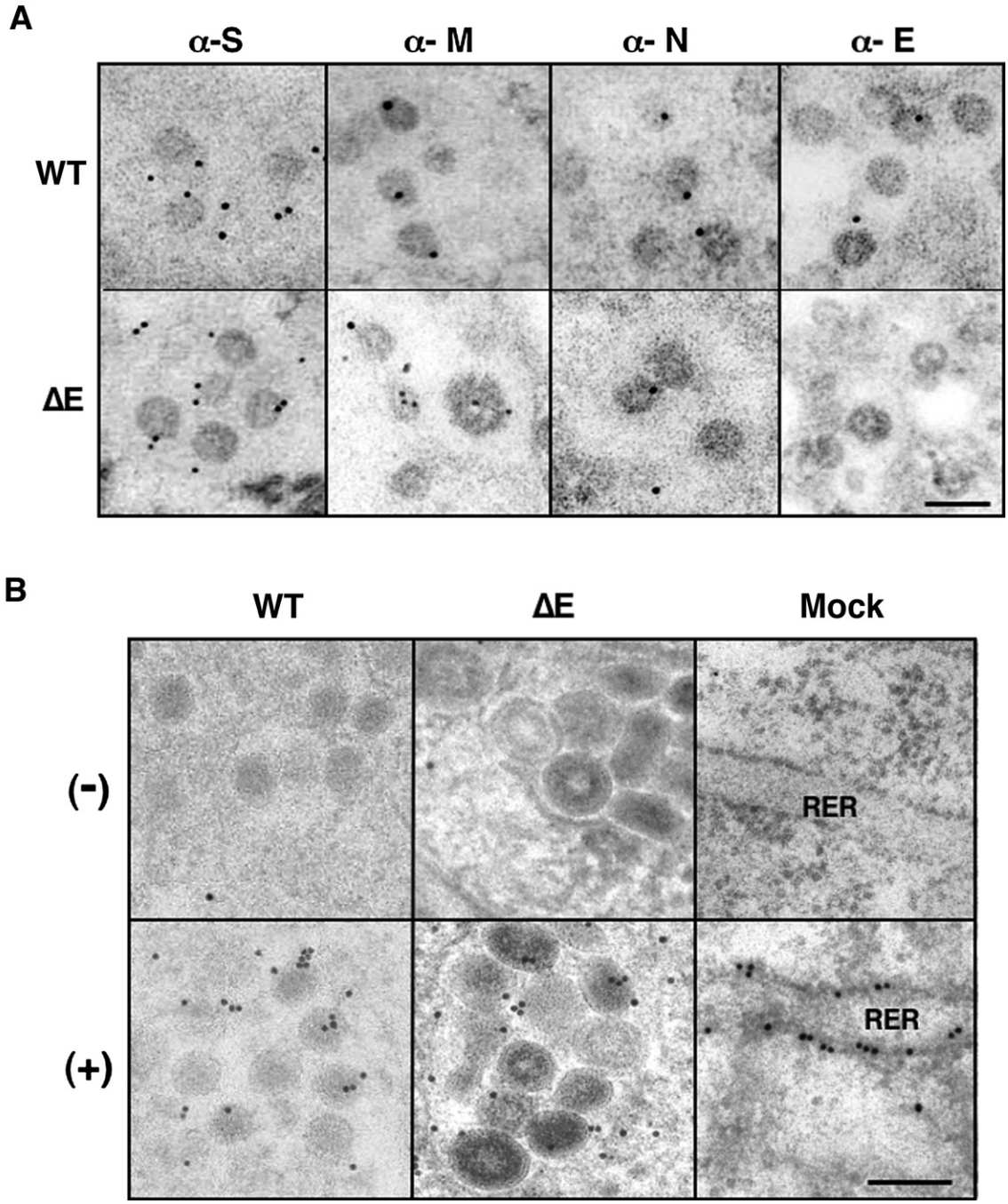

Fig. 3. Characterization of rTGEV-ΔE virions by immunoelectron microscopy. rTGEV-wt (WT) or rTGEV-ΔE (ΔE) infected BHK-pAPN-E$^-$ cells at 24 h p.i. are shown. MAbs specific for the TGEV structural proteins S, M, N, and E (A) and a complex of RNase and colloidal gold (B) were used. Panel A shows samples processed by freeze-substitution in methanol. Panel B shows samples embedded in EML-812. The specificity of RNase-gold labeling (+) was assessed with RNase-treated negative controls (−). Colloidal gold conjugates 10 nm in diameter were used for panels A and B. Scale bars, 100 nm. Mock, non-infected cells. RER, rugose endoplasmic reticulum.

demonstrated that rTGEV-ΔE infected BHK-pAPN-E$^-$ cells did not secrete mature or immature virions.

Immunochemical characterization of rTGEV-ΔE virions

The composition of the large immature viral particles assembled in BHK-pAPN-E$^-$ cells was determined by immunogold detection in sections of freeze-substituted samples. MAbs specific for S, M, and N proteins provided a positive signal on the rTGEV-wt and rTGEV-ΔE virions assembled on BHK-pAPN-E$^-$ cells, whereas only the rTGEV-wt virions bound the MAb specific for E protein, as expected (Fig. 3A).

To study whether rTGEV-ΔE virions incorporated RNA, BHK-pAPN-E$^-$ cells infected with rTGEV-ΔE or rTGEV-wt were analyzed by RNase-gold electron microscopic cytochemistry. RNase-gold complex showed similar binding levels to virions assembled on BHK-pAPN-E$^-$ cells infected with rTGEV-ΔE or rTGEV-wt (Fig. 3B(+)) indicating that the rTGEV-ΔE virions incorporated RNA. Binding of RNase-gold to ribosomes of the rough endoplasmic reticulum (RER) was also clearly observed (Fig. 3B(+)), whereas the RNase-treated negative controls lacked any labeling either on ribosomes or on viral particles (Fig. 3B(−)), confirming binding specificity.

Intracellular localization of TGEV structural proteins in BHK-pAPN-E$^-$ cells infected with rTGEV-ΔE

The intracellular localization of TGEV structural proteins was studied in BHK-pAPN-E$^-$ and E$^+$ cells infected with the rTGEV-ΔE by indirect immunofluorescence using MAbs specific for TGEV S, M, N, and E proteins. The immunofluorescent signal associated with the TGEV structural proteins M, N, and S was similar in BHK-pAPN-E$^-$ and E$^+$ cells (Fig. 4) with some significative differences. Thus, proteins S and M were accumulated in the perinuclear region in infected BHK-pAPN-E$^-$ cells, whereas specific signals for these two proteins were extended to the cytoplasm in infected BHK-pAPN-E$^+$ cells. Immunofluorescence specific for N protein was observed in the cytoplasm of BHK-pAPN-E$^-$ and E$^+$ cells but, in addition, a punctuate immunofluorescence pattern that corresponded to the accumulation of secretory vesicles in late infection stages was also observed in BHK-pAPN-E$^+$ cells (Salanueva et al., 1999). The changes observed in the subcellular localization of the TGEV structural proteins, in the absence of E protein, suggested an arrest in TGEV intracellular transport, whereas in BHK-pAPN-E$^+$ cells rTGEV-ΔE virions progressed through the Golgi to release from the cell by exocytosis.

Previous studies (Salanueva et al., 1999) suggested that TGEV morphological transformation from large immature particles into more condensed mature virus particles takes place during its transport along the exocytic pathway. To determine the effect of E gene deletion on TGEV infection of BHK-pAPN-E$^-$ cells, the subcellular localization of virus particles and endoplasmic reticulum (protein disulfide-isomerase, PDI), intermediate compartment and *cis*-Golgi (KDEL receptor), and *trans*-Golgi (giantin) specific markers were compared by immunofluorescence laser scanning confocal microscopy in rTGEV-wt and rTGEV-ΔE infected BHK-pAPN-E$^-$ and E$^+$ cells at different times post-infection (0, 8, 14, and 24 h post-infection). The immunofluorescence pattern observed with endoplasmic reticulum markers was similar in BHK-pAPN-E$^+$ and E$^-$ cells infected with rTGEV-wt or rTGEV-ΔE, and in non-infected cells, at all the time points analyzed, indicating that the overall distribution of this organelle in the cell cytoplasm was not significantly affected by any of these two viruses (Fig. 5). Only the time points 0 and 24 h are shown for simplicity.

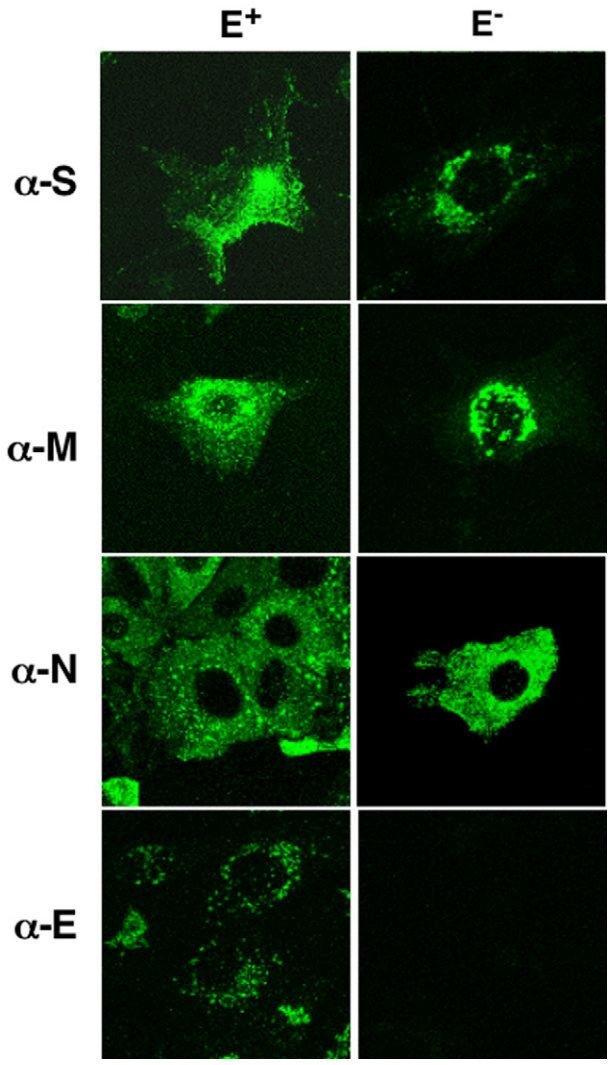

Fig. 4. Detection of TGEV structural proteins in rTGEV-ΔE infected BHK-pAPN-E$^+$ and E$^-$ cells by immunofluorescence. TGEV structural proteins were detected by immunofluorescence using MAbs specific for S, M, N, and E proteins in rTGEV-ΔE infected BHK-pAPN-E$^+$ and E$^-$ cells at 16 h p.i.

KDEL receptor immunofluorescence specific signal in the intermediate compartment and *cis*-Golgi was almost undetectable in rTGEV-wt infected BHK-pAPN-E$^-$ and E$^+$ cells (Fig. 6). In contrast, the KDEL receptor specific signal in BHK-pAPN-E$^-$ cells infected with rTGEV-ΔE showed a progressive and strong accumulation at 24 h post-infection (Fig. 6).

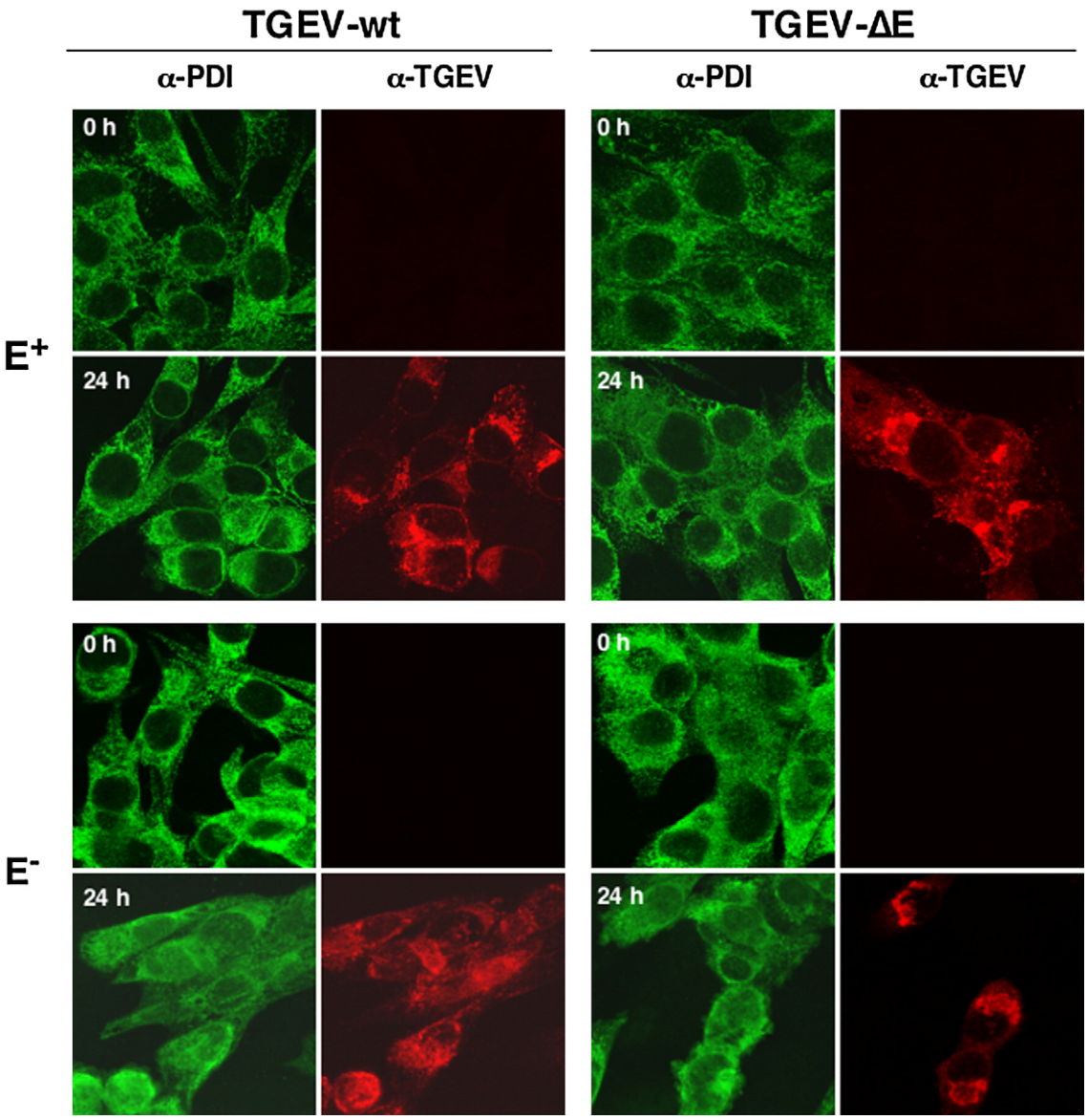

Fig. 5. Detection of the endoplasmic reticulum marker PDI and rTGEV in BHK-pAPN-E^+ and E^- cells by immunofluorescence. TGEV infection and protein disulfide isomerase (PDI) were monitored in BHK-pAPN-E^+ and E^- cells infected with rTGEV-wt and rTGEV-ΔE at 0 and 24 h p.i. by immunofluorescence microscopy using a rabbit polyclonal antibody specific for PDI and a TGEV M protein specific MAb.

Immunoblots were performed and an increase in the amount of KDEL-R was observed in rTGEV-ΔE infected E^- cells, consistent with the result obtained by confocal microscopy (data not shown). Similar effect has been described (Salanueva et al., 1999) when TGEV infection is blocked with monensin, a drug that selectively affects the Golgi complex interrupting the secretory pathway (data not shown). Furthermore, the infection with rTGEV-ΔE in presence of E protein provided in trans showed no accumulation of KDEL receptor (Fig. 6). These data indicated that the accumulation of ERGIC vesicles could be a consequence of a membrane trafficking blockade in the secretory pathway leading to the inhibition of TGEV morphogenesis in the absence of E protein.

Staining for the Golgi complex in approximately 90% of rTGEV-wt infected BHK-pAPN-E^+ and E^- cells showed fragmentation and dispersion of Golgi membranes at 24 h post-infection (Fig. 7), whereas this disruption of Golgi was observed in only 20% of rTGEV-ΔE infected BHK-pAPN-E^+ cells at 24 h post-infection probably due to the delay in the infection progress. In fact, later in the infection, the disruption Golgi was up to 100% in rTGEV-ΔE infected BHK-pAPN-E^+ (data not shown). In contrast, disorganization of Golgi was not observed in rTGEV-ΔE infected BHK-pAPN-E^- cells at the analyzed times, indicating that the virus maturation did not progress from ERGIC to *trans*-Golgi in the absence of E protein. Taken together, these data indicate an arrest in the virus maturation in ERGIC, which is the TGEV budding compartment (Salanueva et al., 1999).

To confirm that the virus particles were blocked in the ERGIC in the absence of E protein, immunoelectron microscopy was developed to analyze the markers of the membrane-bound compartments containing virus particles. A different

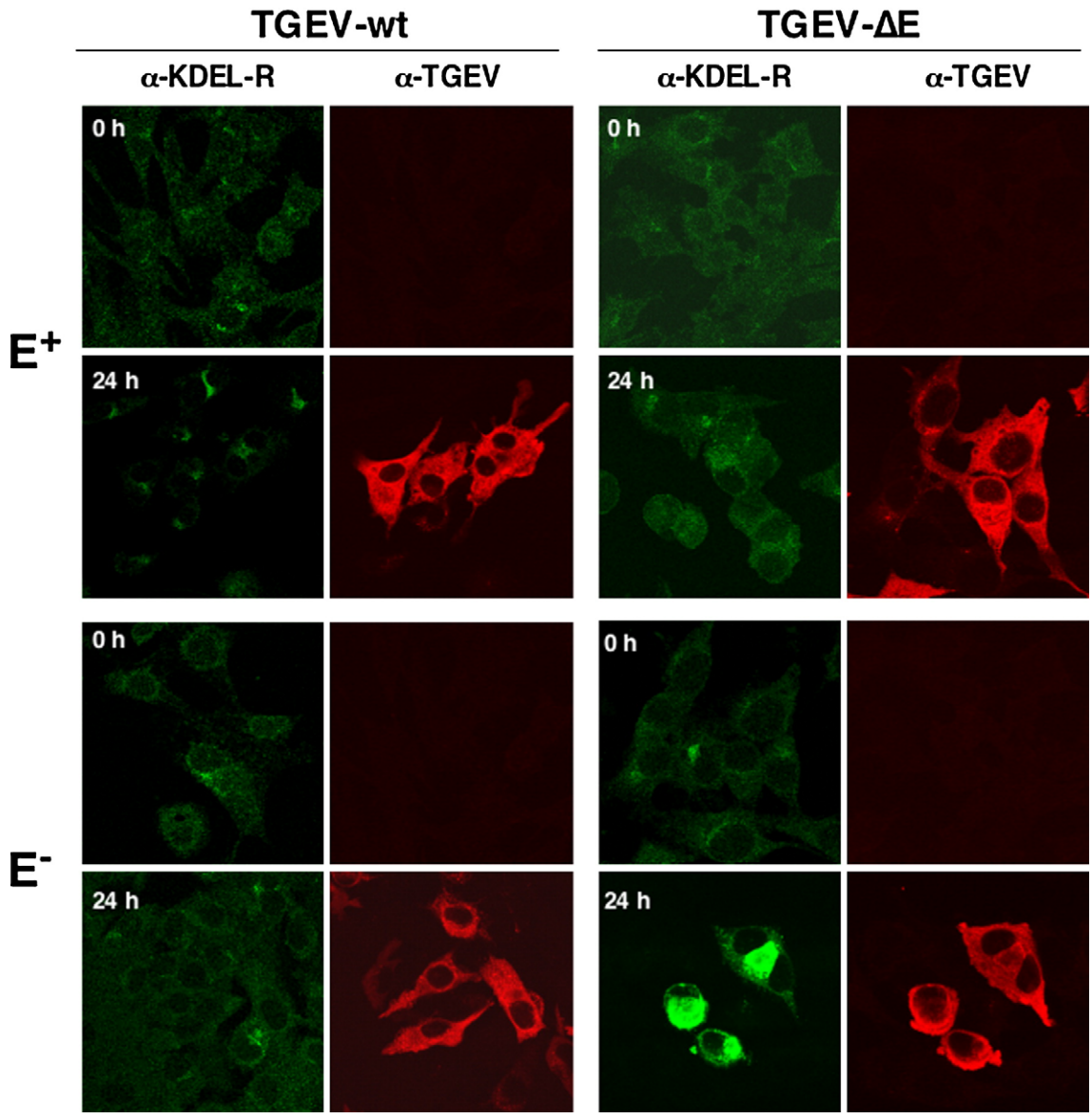

Fig. 6. Detection of KDEL-R and rTGEV in BHK-pAPN-E^+ and E^- cells by immunofluorescence. TGEV infection and the ERGIC marker KDEL-R were monitored in BHK-pAPN-E^+ and E^- cells infected with rTGEV-wt and rTGEV-ΔE at 0 and 24 h p.i. by immunofluorescence microscopy using a rabbit polyclonal antibody specific for TGEV and a KDEL-R specific MAb.

specific marker for the intermediate compartment, ERGIC-53/p58, was used due to the reduced signal observed for KDEL-R. The antibody specific for ERGIC-53/p58 provided a positive signal on the vesicles containing rTGEV-ΔE virions assembled on ST-E^- cells (Figs. 8A and B), whereas cytoplasm areas without virus vesicles and nucleus lacked any labeling, confirming the antibody binding specificity (Figs. 8A and C).

Discussion

It has been shown that E protein is essential for TGEV morphogenesis. In TGEV-ΔE infected BHK-pAPN-E^- cells virions containing RNA were assembled, virus transportation was arrested in the ERGIC and full virus maturation was blocked and mature infectious virus was not secreted to the extracellular medium.

Previous studies have shown that, in the group 2 coronavirus MHV and SARS-CoV (DeDiego et al., 2007; Kuo et al., 2002; Kuo and Masters, 2003), E protein is not essential for virus replication, although ΔE defective mutants have a reduced growth in cell culture and in animal models. In contrast, for group 1 coronavirus TGEV, we and others (Curtis et al., 2002; Ortego et al., 2002) have shown that cells transfected with an E gene-deleted TGEV infectious cDNA do not produce infectious virus. Similarly, a gene E knockout mutant of the arterivirus equine arteritis virus (EAV), is unable to produce infectious progeny (Snijder et al., 1999). Kuo and Masters have suggested that the apparent lethality of E gene knockouts in EAV and TGEV may reflect a slow infection kinetics of these viruses that would allow uninfected cells to overgrow infected cells and obscure the detection of ΔE mutants of some nidovirus (Kuo and Masters, 2003). Our results clearly showed, in this and in a

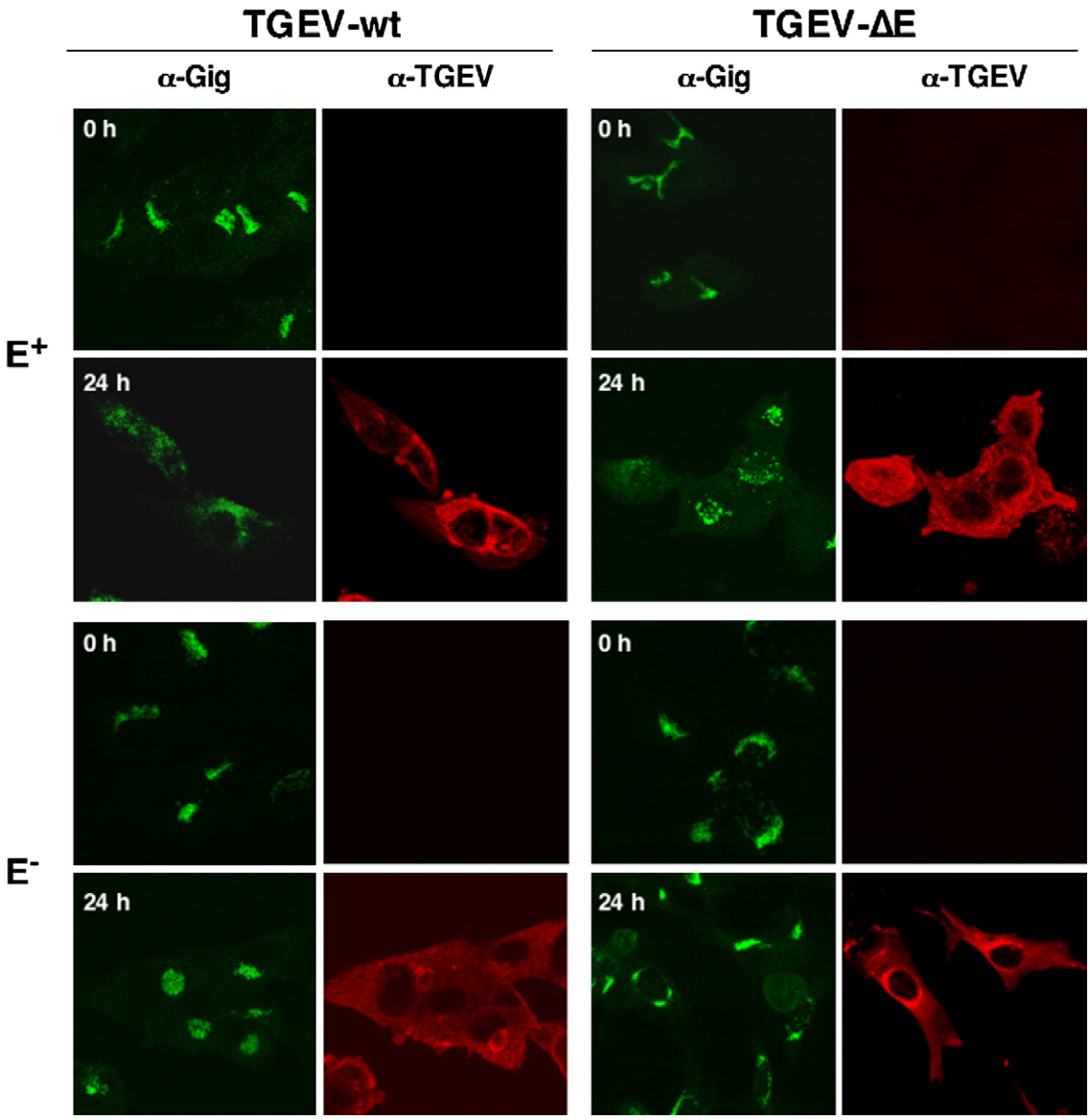

Fig. 7. Detection of giantin and rTGEV in BHK-pAPN-E$^+$ and E$^-$ cells by immunofluorescence. TGEV infection and the Golgi apparatus marker giantin (gig) were monitored in BHK-pAPN-E$^+$ and E$^-$ cells infected with rTGEV-wt and rTGEV-ΔE at 0 and 24 h p.i. by immunofluorescence microscopy using a rabbit polyclonal antibody TGEV specific and a giantin specific MAb.

previous publication (Ortego et al., 2002), that E protein is essential for TGEV replication and that no infectious virus was produced at all. A simple explanation is that these viruses belong to different CoV groups and have different assembly requirements. The generation of infectious rTGEV-ΔE virus was dependent on E protein expression and independent of the infected cell line. Thus, rTGEV-ΔE infected cells did not secrete virus to the extracellular medium, and the virus did not spread to neighboring uninfected cells, and therefore did not generate plaques in infected ST-E$^-$ cells up to 96 h post-infection, confirming that rTGEV-ΔE is a propagation-deficient virus in the absence of E protein provided in trans. Furthermore, no virus amplification was observed using supernatants or cell extracts from BHK-pAPN-E$^-$ cells infected with rTGEV-ΔE virus when used to infect fresh BHK-pAPN-E$^+$ cells, although these cells could have amplified minute amounts of rTGEV-ΔE virus. These data confirmed that E protein was essential for TGEV virus replication. Therefore, a different behavior is shown by coronavirus from groups 1 and 2 in the requirement for E protein during virus assembly.

The requirement of E and M proteins for the formation of virus-like particles has been previously described (Vennema et al., 1996). Co-infection with recombinant baculoviruses showed that the membrane and envelope proteins are sufficient for the efficient formation of coronavirus VLPs (Mortola and Roy, 2004). In contrast, Huang and coworkers reported that two viral genes, encoding the SARS-CoV M and N proteins, are necessary and sufficient for formation of VLPs by cotransfection of expression plasmids (Huang et al., 2004). This discrepancy could be explained by the different cell types used in these studies (insect S*f*9 and human 293T cells, respectively). In our study, electron microscopy analysis of BHK-pAPN-E$^-$ cells

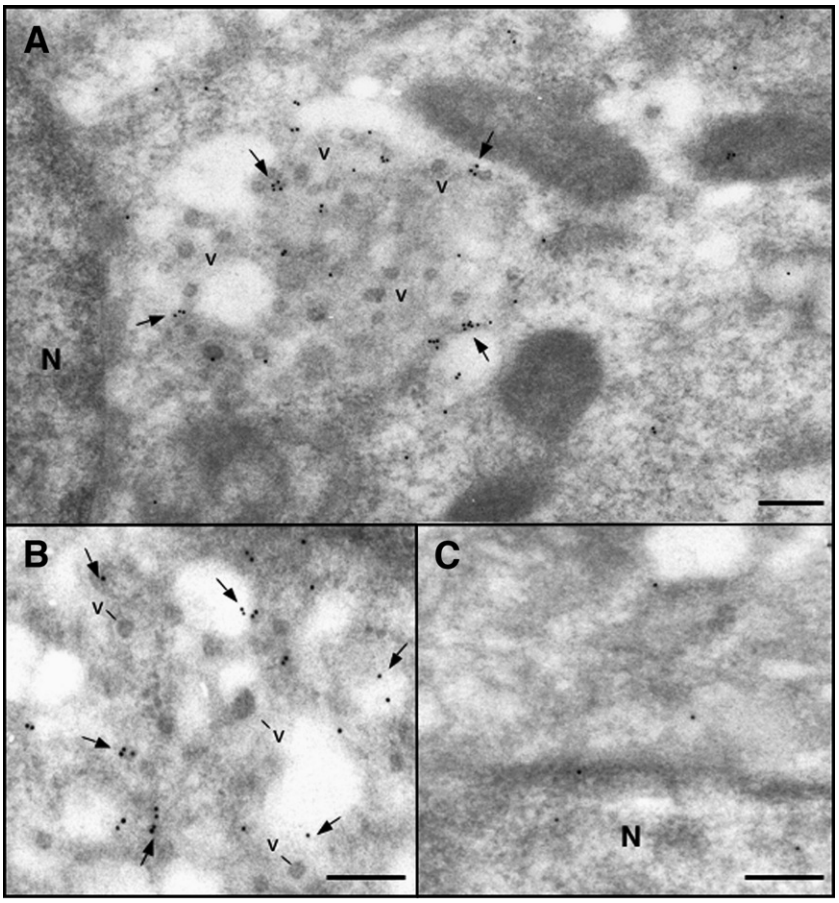

Fig. 8. Immunoelectron microscopy of ERGIC in rTGEV-ΔE infected ST-E$^-$ cells. Panel A and B show vesicles filled with viruses that react with the anti-ERGIC-53/p58 antibody, specific marker for the intermediate compartment. Panel C shows a detail of the cytoplasm and nucleus where ERGIC-53/p58 specific signal was not observed. ERGIC-53/p58 specific signal is indicated with arrows. v, viruses; N, nucleus. Scale bars, 100 nm.

infected with rTGEV-ΔE demonstrated that only immature TGEV virions were assembled in the absence of E protein. These virions contained RNA, and also all the structural TGEV proteins (S, M, and N) except the deleted E protein. These results indicate that the E protein is essential for the formation of mature TGEV virions. In the absence of E protein, the assembled virions displayed a morphology different from the full-length virus, were non-infectious, accumulated in the cytoplasm of the infected cells, and were not released to the extracellular medium or transported to neighboring cells.

TGEV replication depends on the exocytic pathway to complete its morphogenesis (Salanueva et al., 1999). Virions were assembled as large particles with annular morphology at perinuclear compartment of the cells, and changed their morphology into small dense virions during the transport along the exocytic route (Risco et al., 1998; Tooze et al., 1987). In cells infected with rTGEV-ΔE, an accumulation of the KDEL receptor and the lack of fragmentation and dispersion of Golgi membranes were observed in absence of E protein. These effects and rTGEV-ΔE virus assembly into mature particles were recovered by providing E protein in trans. In addition, immunoelectron microscopy studies with an intermediate compartment specific marker confirmed that, in the absence of the E protein, the maturation of the virus is arrested in the ERGIC. A similar effect has been described when TGEV infection is blocked with monensin, a drug that selectively affects the Golgi complex interrupting the secretory pathway. Monensin blocks the viral transport from ERGIC, leading to the accumulation of numerous large viral particles in dilated pre-Golgi ERGIC elements of vacuolar morphology (Salanueva et al., 1999). The comparable deficiencies observed in viral morphogenesis in the absence of E protein and as a result of treatment with monensin suggest an aberrant assembly process due to the absence of E protein. In principle, E protein could act directly on the ERGIC and Golgi compartments, on the virus itself, or in both. It has been postulated that E protein prepares the membrane or other viral proteins occupying strategic positions within the budding pathways (Salanueva et al., 1999), as proposed for small acylated glycoproteins of alphaviruses and orthomyxoviruses that also display ion channel activity (Gaedigk-Nitschko et al., 1990; Ivanova et al., 1995; Liao et al., 2006; Wilson et al., 2004; Zebedee and Lamb, 1988). The absence of E protein would inhibit the progression through the ERGIC-Golgi compartments, resulting in the accumulation of virions in the ERGIC and of the ERGIC itself.

E proteins from MHV and SARS-CoV have viroporin activity (Liao et al., 2004; Madan et al., 2005). Viroporins act at late stages of the viral cycle promoting the exit of new virus

particles from the cell (Gonzalez and Carrasco, 2003). The exact mechanism by which viroporins alter the permeability of the plasma membrane is unknown, and it is possible that this activity is displayed both at the plasma membrane and on cellular organelles (Aldabe et al., 1997; Van kuppeveld et al., 1997). Coronavirus E protein localizes in membranes of ERGIC, where it could modify their permeability, leading to the disruption of ion gradients at intracellular organelles (Madan et al., 2005), facilitating the transport of the virions along the exocytic pathway and their maturation. The absence of this viroporin activity mediated by the E protein possibly leads to the arrest of the transport of virions through the secretory pathway, the accumulation of non-mature virions in ERGIG, and the absence of release of new infectious virus from the cell. The construction of E protein mutants affecting E protein ion channel activity could assess whether this postulate is correct.

E proteins from the different coronavirus groups show different channel selectivity. The E protein from the group 1 coronavirus HCoV-229E is K^+ selective, whereas from the group 2 MHV and SARS-CoV, and group 3 coronavirus IBV, E protein is Na^+ selective (Wilson et al., 2006, 2004). The diverse channel selectivity among the coronavirus groups could be translated in differences in the effect of E protein in the secretory pathway and may explain the discrepancies among the gene E-defective mutants from the three coronavirus groups, and why E protein is essential for replication of group 1 viruses and non-essential for replication of group 2 viruses. Additional analysis of the gene E-defective mutants during assembly is required to shed light on the functions of the E protein in coronavirus morphogenesis in the three virus groups of the *Coronaviridae* family.

In conclusion, the arrest of TGEV maturation and the accumulation of virions in the secretory pathway due to the absence of the E protein confirm that this protein is essential for TGEV transportation and morphogenesis. The ability to generate TGEV-ΔE mutants that are replication-competent but propagation-deficient by complementation in packaging cell lines, supports the potential use of these mutants as vaccine vectors.

Materials and methods

Virus and cells

Recombinant rTGEV-*Mlu*I–*Fse*I (rTGEV-wt) and rTGEV-Δ3abΔE (rTGEV-ΔE) (Ortego et al., 2002, 2003) were grown as described (Jiménez et al., 1986). Baby hamster cells (BHK-21) stably transformed with the gene coding for the porcine aminopeptidase N (BHK-pAPN) (Delmas et al., 1992) were grown in Dulbecco's modified Eagle's medium (DMEM) supplemented with 2% fetal calf serum (FCS) containing Geneticin G418 (1.5 mg/ml) as a selector agent. Porcine kidney cells, LLC-PK1 (European Collection of Cell cultures no. 86121112), were grown in medium 199 supplemented with 2 mM glutamine and 10% FCS. Cat kidney cells, CRFK (ATCC CCL 94), were grown in DMEM supplemented with 2% FCS. BHK-pAPN-E^+ and LLC-PK1-E^+ cells were grown as described previously (Ortego et al., 2002). Standard virus titrations were performed in porcine swine testis (ST) cells. Titrations of virus with the E gene deleted were performed in LLC-PK1 cells expressing the E protein.

Antibodies

The murine MAbs 1D.G3, 3B.B3, and 3B.D10, specific for TGEV S, M, and N proteins, respectively, have been previously described (Gebauer et al., 1991; Risco et al., 1995; Sánchez et al., 1990). The murine MAb Q3, specific for TGEV E protein, was a kind gift of H. Laude (INRA, Jouy-en Josas, France). The rabbit serum specific for PDI and the murine MAb specific for giantin was generously provided by A. Nieto (Centro Nacional de Biotecnología, CSIC, Madrid, Spain) and M. Renz (Institute of Immunology and Molecular Genetics, Karlsruhe, Germany), respectively. The murine MAb specific for KDEL receptor and the rabbit polyclonal antibody specific for ERGIC-53/p58 were purchased from Stressgen Biotechnologies Corp. (Victoria, BC, Canada) and Sigma-Aldrich (St. Louis. MO, USA), respectively.

TGEV virion purification

TGEV virions were sedimented through a 20% sucrose cushion in TEN (Tris–HCl 10 mM [pH 7.4], EDTA 1 mM, NaCl 1M) 0.2% Tween 20 by centrifugation in an SW28 Beckman rotor at 25,000 rpm for 2 h at 4 °C. Sucrose was removed and the pellet was washed with TEN. Pellet was recovered by suspending it in TEN-0.2% Tween 20 and sedimented by centrifugation in a SW 41 Beckman rotor for 1 h at 25,000 rpm. Virions were recovered by suspending the pellet in TNE (Tris–HCl 10 mM [pH 7.4], EDTA 1 mM, NaCl 100 mM) and analyzed by sodium dodecyl sulfate-polyacrylamide gel electrophoresis (SDS-PAGE) and silver staining or negative staining and electron microscopy.

Electron microscopy

Processing of infected cells for embedding in EML-812 for ultrastructural studies

Monolayers of BHK-pAPN cells expressing TGEV E protein and control cells were infected with rTGEV-*wt* or rTGEV-ΔE virus. The cells were fixed in situ at 12, 16, and 24 h post-infection with a mixture of 2% glutaraldehyde and 1% tannic acid in 0.4 M HEPES buffer (pH 7.2) for 2 h at room temperature. The fixed monolayers were removed from the dishes in the fixative and transferred to Eppendorf tubes. After centrifugation in a microcentrifuge, the cell pellets were washed with HEPES buffer and processed for embedding in EML-812 (Taab Laboratories, Berkshire, United Kingdom) as described (Risco et al., 1998). The cells were post-fixed with a mixture of 1% osmium tetroxide and 0.8% potassium ferricyanide in distilled water for 1 h at 4 °C. After four washes with HEPES buffer, samples were incubated with 2% uranyl acetate, washed again, and dehydrated in increasing concentrations of acetone (50, 70, 90, and 100%) for 15 min each at 4 °C. Infiltration in the resin EML-812 was done at room temperature for 1 day. Polymerization of infiltrated samples was done at 60 °C for

2 days. Ultrathin (50- to 60-nm-thick) sections of the samples were stained with saturated uranyl acetate and lead citrate by standard procedures.

Quick freezing and freeze-substitution of cells

Cultures of cells were subjected to a mild fixation with a solution of 4% paraformaldehyde containing 0.1% glutaraldehyde in PBS at 4 °C for 30 min. Small pellets of chemically fixed cells were cryoprotected with glycerol, applied to small pieces of filter paper, blotted, and quick frozen in liquid ethane. Vitrified specimens were transferred to a Reichert-Jung AFS freeze-substitution unit (Leica, Vienna, Austria) and maintained for 48 h at −90 °C in a mixture of methanol and 0.5% (w/v) uranyl acetate. After freeze-substitution, samples were infiltrated in Lowicryl K4M (EML Laboratories) at −30 °C and polymerized with UV light. Ultrathin sections of the samples were either stained or processed for immunogold labeling.

Immunoelectron microscopy

Immunogold detection of TGEV proteins on ultrathin-sections of infected BHK-pAPN cells was performed at room temperature with MAbs specific for M, N, S, E, and ERGIC-53 proteins by established procedures (Risco et al., 1995). Sections collected on Formvar coated gold electron microscopy grids were incubated for 30 min with Tris buffer-gelatin and then floated on drops of diluted primary antibodies for 75 min. After jet washing with PBS, samples were incubated for 45 min with secondary antibodies conjugated with 10-nm-diameter gold particles and washed again with PBS and distilled water. Samples were then allowed to dry on filter paper before being stained with saturated uranyl acetate for 25 min, followed by 1 min with lead citrate. All samples were analyzed with a JEOL 1200 EX II electron microscope.

For ultrastructural detection of RNA, a complex of RNase and 10-nm-diameter colloidal gold (EY Laboratories, San Diego, CA) was used as described previously (Risco et al., 1998). Ultrathin sections from Epon-included samples were collected on gold electron microscopy (EM) grids covered with collodion and incubated for 40 min at room temperature with the gold conjugated RNase diluted 1:20 in PBS. After being washed with PBS and distilled water, samples were stained with uranyl acetate and lead citrate. To unmask viral RNA molecules, sections were subjected to a treatment before incubation with RNase-gold consisting on 15 min incubation at 37 °C with proteinase K (10 μg/ml in Tris-EDTA), washing with TE, 10 min fixation with 4% paraformaldehyde in PBS, washing again with PBS, and incubation for 10 min with 0.2 M NH_4Cl. As a cytochemical control, some sections were pre-incubated for 30 min at 37 °C with a solution of non-conjugated RNase (20 μg/ml) before being treated with the RNase-gold conjugated.

Negative staining of rTGEV-ΔE virions

Virus from supernatants of BHK-pAPN-E^+ and E^- cells infected with rTGEV-ΔE virus, concentrated 200-fold, were analyzed by negative staining as described (Bremer et al., 1998). Briefly, samples were adsorbed to UV light-activated copper grids for 2 min at room temperature. Grids were washed two times in H_2O (Escors et al., 2001) and stained with 2% uranyl acetate for 1 min. Samples were visualized in a JEOL 1200 EXII transmission electron microscope.

Immunofluorescence

Cells were plated on glass coverslips. Infections were performed at an m.o.i. = 1 pfu/cell at 37 °C in DMEM containing 2% FCS. The inoculum was removed at 90 min and the cells were maintained in DMEM 2% FCS. At the times indicated, cells were washed with PBS and fixed by addition of 4% paraformaldehyde for 30 min at room temperature. For dual-labeling experiments in which, one primary antibody was derived from mouse and the other one from rabbit, both antibodies were combined in a PBS-FCS 20% diluent containing 0.2% Saponin (Superfos-Biosector, Vedback, Denmark). Antibodies were allowed to adsorb for 90 min at room temperature, and washed three times with PBS-FCS 2%. Cells were then incubated for 30 min at room temperature with a mixture of anti-rabbit and anti-mouse secondary antibodies conjugated to Alexa 488 or Alexa 594. The coverslips were washed five times with PBS-FCS 2%, mounted on glass slides, and analyzed with a Laser Scanning Confocal System Radiance 2100 (Bio-Rad) on a Zeiss Axiovert 200 microscope. Argon ion and He–Ne lasers at 488 and 543 nm were employed as excitation sources. Image acquisition was performed using LaserSharp2000 v.5 software.

Acknowledgments

We thank S. Zuñiga, I. Sola, J.L. Moreno, M.L DeDiego, and E. Alvarez for critically reading the manuscript and helpful discussions. We are also grateful to D. Dorado, and R. Arranz for their excellent technical assistance. This work was supported by grants from the Comisión Interministerial de Ciencia y Tecnología (CICYT), the Consejería de Educación y Cultura de la Comunidad de Madrid, Fort Dodge Veterinaria, and the European Communities (Projects FMDV Vaccine. QRLT-2001-00825 and DISSECT, SP22-CT-2004-511060).

References

Aldabe, R., Irurzun, A., Carrasco, L., 1997. Poliovirus protein 2BC increases cytosolic free calcium concentrations. J. Virol. 71, 6214–6217.

Almazán, F., González, J.M., Pénzes, Z., Izeta, A., Calvo, E., Plana-Durán, J., Enjuanes, L., 2000. Engineering the largest RNA virus genome as an infectious bacterial artificial chromosome. Proc. Natl. Acad. Sci. USA 97, 5516–5521.

Arbely, E., Khattari, Z., Brotons, G., Akkawi, M., Salditt, T., Arkin, I.T., 2004. A highly unusual palindromic transmembrane helical hairpin formed by SARS coronavirus E protein. J. Mol. Biol. 341, 769–779.

Baudoux, P., Carrat, C., Besnardeau, L., Charley, B., Laude, H., 1998. Coronavirus pseudoparticles formed with recombinant M and E proteins induce alpha interferon synthesis by leukocytes. J. Virol. 72, 8636–8643.

Bremer, A., Häner, M., Aebi, U., 1998. Negative staining, Second ed. In: Celis, E. (Ed.), Cell Biology. A Laboratory Handbook, vol. 3. Academic Press, San Diego, pp. 277–284.

Brierley, I., Digard, P., Inglis, S.C., 1989. Characterization of an efficient

coronavirus ribosomal frameshifting signal: requirement for an RNA pseudoknot. Cell 57, 537–547.
Casais, R., Thiel, V., Siddell, S.G., Cavanagh, D., Britton, P., 2001. Reverse genetics system for the avian coronavirus infectious bronchitis virus. J. Virol. 75, 12359–12369.
Corse, E., Machamer, C.E., 2000. Infectious bronchitis virus E protein is targeted to the Golgi complex and directs release of virus-like particles. J. Virol. 74, 4319–4326.
Curtis, K.M., Yount, B., Baric, R.S., 2002. Heterologous gene expression from transmissible gastroenteritis virus replicon particles. J. Virol. 76, 1422–1434.
DeDiego, M.L., Alvarez, A., Almazan, F., Rejas, M.T., Lamirande, E., Roberts, A., Shieh, W.J., Zaki, S., Subbarao, K., Enjuanes, L., 2007. A severe acute respiratory syndrome coronavirus that lacks the E gene is attenuated in vitro and in vivo. J. Virol. 81, 1701–1713.
Delmas, B., Gelfi, J., L'Haridon, R., Vogel, L.K., Norén, O., Laude, H., 1992. Aminopeptidase N is a major receptor for the enteropathogenic coronavirus TGEV. Nature 357, 417–420.
Enjuanes, L., Brian, D., Cavanagh, D., Holmes, K., Lai, M.M.C., Laude, H., Masters, P., Rottier, P., Siddell, S.G., Spaan, W.J.M., Taguchi, F., Talbot, P., 2000a. *Coronaviridae*. In: Wickner, R.B. (Ed.), Virus taxonomy. Classification and Nomenclature of Viruses. Academic Press, San Diego, California, pp. 835–849.
Enjuanes, L., Spaan, W., Snijder, E., Cavanagh, D., 2000b. Nidovirales. In: Wickner, R.B. (Ed.), Virus Taxonomy. Classification and Nomenclature of Viruses. Academic Press, San Diego, California, pp. 827–834.
Escors, D., Camafeita, E., Ortego, J., Laude, H., Enjuanes, L., 2001. Organization of two transmissible gastroenteritis coronavirus membrane protein topologies within the virion and core. J. Virol. 75, 12228–12240.
Esper, F., Shapiro, E.D., Weibel, C., Ferguson, D., Landry, M.L., Kahn, J.S., 2005a. Association between a novel human coronavirus and Kawasaki disease. J. Infect. Dis. 191, 499–502.
Esper, F., Weibel, C., Ferguson, D., Landry, M.L., Kahn, J.S., 2005b. Evidence of a novel human coronavirus that is associated with respiratory tract disease in infants and young children. J. Infect. Dis. 191, 492–498.
Gaedigk-Nitschko, K., Ding, M.X., Levy, M.A., Schlesinger, M.J., 1990. Site-directed mutations in the Sindbis virus 6K protein reveal sites for fatty acylation and the underacylated protein affects virus release and virion structure. Virology 175, 282–291.
Gebauer, F., Posthumus, W.A.P., Correa, I., Suñé, C., Sánchez, C.M., Smerdou, C., Lenstra, J.A., Meloen, R., Enjuanes, L., 1991. Residues involved in the formation of the antigenic sites of the S protein of transmissible gastroenteritis coronavirus. Virology 183, 225–238.
Godet, M., L'Haridon, R., Vautherot, J.F., Laude, H., 1992. TGEV coronavirus ORF4 encodes a membrane protein that is incorporated into virions. Virology 188, 666–675.
Gonzalez, M.E., Carrasco, L., 2003. Viroporins. FEBS Lett. 552, 28–34.
Hertzig, T., Sacandella, E., Schelle, B., Ziebuhr, J., Siddell, S., Ludewig, B., Thiel, V., 2004. Rapid identification of coronavirus replicase inhibitors using a selectable replicon RNA. J. Gen. Virol. 85, 1717–1725.
Hsieh, P.K., Chang, S.C., Huang, C.C., Lee, T.T., Hsiao, C.W., Kou, Y.H., Chen, I.Y., Chang, C.K., Huang, T.H., Chang, M.F., 2005. Assembly of severe acute respiratory syndrome coronavirus RNA packaging signal into virus-like particles is nucleocapsid dependent. J. Virol. 79, 13848–13855.
Huang, Y., Yang, Z.Y., Kong, W.P., Nabel, G.J., 2004. Generation of synthetic severe acute respiratory syndrome coronavirus pseudoparticles: implications for assembly and vaccine production. J. Virol. 78, 12557–12565.
Ivanova, L., Lustig, S., Schlesinger, M.J., 1995. A pseudo-revertant of a Sindbis virus 6K protein mutant, which corrects for aberrant particle formation, contains two new mutations that map to the ectodomain of the E2 glycoprotein. Virology 206, 1027–1034.
Jiménez, G., Correa, I., Melgosa, M.P., Bullido, M.J., Enjuanes, L., 1986. Critical epitopes in transmissible gastroenteritis virus neutralization. J. Virol. 60, 131–139.
Kapke, P.A., Brian, D.A., 1986. Sequence analysis of the porcine transmissible gastroenteritis coronavirus nucleocapsid protein gene. Virology 151, 41–49.
Koetzner, C.A., Parker, M.M., Ricard, C.S., Sturman, L.S., Masters, P.S., 1992. Repair and mutagenesis of the genome of a deletion mutant of the coronavirus mouse hepatitis virus by targeted RNA recombination. J. Virol. 66, 1841–1848.
Kuiken, T., Fouchier, R.A.M., Schutten, M., Rimmelzwaan, G.F., van Amerongen, G., van Riel, D., Laman, J.D., de Jong, T., van Doornum, G., Lim, W., Ling, A.E., Chan, P.K.S., Tam, J.S., Zambon, M.C., Gopal, R., Drosten, C., van der Werf, S., Escriou, N., Manuguerra, J.-C., Stohr, K., Peiris, J.S.M., 2003. Newly discovered coronavirus as the primary cause of severe acute respiratory syndrome. Lancet 362, 263–270.
Kuo, L., Masters, P.S., 2003. The small envelope protein E is not essential for murine coronavirus replication. J. Virol. 77, 4597–4608.
Kuo, L., Godeke, G.-J., Raamsman, M.J.B., Masters, P.S., Rottier, P.J.M., 2000. Retargeting of coronavirus by substitution of the spike glycoprotein ectodomain: crossing the host cell species barrier. J. Virol. 74, 1393–1406.
Kuo, L., Hurst, R., Masters, P.S., 2002. 21st Annual Meeting, Lexington, Kentucky.
Kuo, L., Hurst, K.R., Masters, P., 2007. Exceptional flexibility in the sequence requirements for coronavirus small envelope protein function. J. Virol. 81, 2249–2262.
Lewicki, D.N., Gallagher, T.M., 2002. Quaternary structure of coronavirus spikes in complex with carcinoembryonic antigen-related cell adhesion molecule cellular receptors. J. Biol. Chem. 277, 19727–19734.
Liao, Y., Lescar, J., Tam, J.P., Liu, D.X., 2004. Expression of SARS-coronavirus envelope protein in *Escherichia coli* cells alters membrane permeability. Biochem. Biophys. Res. Commun. 325, 374–380.
Liao, Y., Yuan, Q., Torres, J., Tam, J.P., Liu, D.X., 2006. Biochemical and functional characterization of the membrane association and membrane permeabilizing activity of the severe acute respiratory syndrome coronavirus envelope protein. Virology 349, 264–275.
Liu, D.X., Inglis, S.C., 1991. Association of the infectious bronchitis virus-3c protein with the virion envelope. Virology 185, 911–917.
Madan, V., Garcia M de, J., Sanz, M.A., Carrasco, L., 2005. Viroporin activity of murine hepatitis virus E protein. FEBS Lett. 579, 3607–3612.
Maeda, J., Maeda, A., Makino, S., 1999. Release of coronavirus E protein membrane vesicles form virus-infected cells and E protein-expressing cells. Virology 263, 265–272.
Masters, P.S., 1999. Reverse genetics of the largest RNA viruses. Adv. Virus Res. 53, 245–264.
Mortola, E., Roy, P., 2004. Efficient assembly and release of SARS coronavirus-like particles by a heterologous expression system. FEBS Lett. 576, 174–178.
Narayanan, K., Makino, S., 2001. Cooperation of an RNA packaging signal and a viral envelope protein in coronavirus RNA Packaging. J. Virol. 75, 9059–9067.
Ortego, J., Escors, D., Laude, H., Enjuanes, L., 2002. Generation of a replication-competent, propagation-deficient virus vector based on the transmissible gastroenteritis coronavirus genome. J. Virol. 76, 11518–11529.
Ortego, J., Sola, I., Almazan, F., Ceriani, J.E., Riquelme, C., Balasch, M., Plana-Durán, J., Enjuanes, L., 2003. Transmissible gastroenteritis coronavirus gene 7 is not essential but influences in vivo virus replication and virulence. Virology 308, 13–22.
Penzes, Z., González, J.M., Calvo, E., Izeta, A., Smerdou, C., Mendez, A., Sánchez, C.M., Sola, I., Almazán, F., Enjuanes, L., 2001. Complete genome sequence of transmissible gastroenteritis coronavirus PUR46-MAD clone and evolution of the Purdue virus cluster. Virus Genes 23, 105–118.
Raamsman, M.J.B., Locker, J.K., de Hooge, A., de Vries, A.A.F., Griffiths, G., Vennema, H., Rottier, P.J.M., 2000. Characterization of the coronavirus mouse hepatitis virus strain A59 small membrane protein E. J. Virol. 74, 2333–2342.
Risco, C., Antón, I.M., Suñé, C., Pedregosa, A.M., Martín-Alonso, J.M., Parra, F., Carrascosa, J.L., Enjuanes, L., 1995. Membrane protein molecules of transmissible gastroenteritis coronavirus also expose the carboxy-terminal region on the external surface of the virion. J. Virol. 69, 5269–5277.
Risco, C., Muntión, M., Enjuanes, L., Carrascosa, J.L., 1998. Two types of virus-related particles are found during transmissible gastroenteritis virus morphogenesis. J. Virol. 72, 4022–4031.
Rottier, P.J.M., 1995. The coronavirus membrane glycoprotein. In: Siddell, S.G. (Ed.), The Coronavirus. Plenum press, New York, pp. 115–135.

Salanueva, I.J., Carrascosa, J.L., Risco, C., 1999. Structural maturation of the transmissible gastroenteritis coronavirus. J. Virol. 73, 7952–7964.

Sánchez, C.M., Jiménez, G., Laviada, M.D., Correa, I., Suñé, C., Bullido, M.J., Gebauer, F., Smerdou, C., Callebaut, P., Escribano, J.M., Enjuanes, L., 1990. Antigenic homology among coronaviruses related to transmissible gastroenteritis virus. Virology 174, 410–417.

Shen, X., Xue, J.H., Yu, C.Y., Luo, H.B., Qin, L., Yu, X.J., Chen, J., Chen, L.L., Xiong, B., Yue, L.D., Cai, J.H., Shen, J.H., Luo, X.M., Chen, K.X., Shi, T.L., Li, Y.X., Hu, G.X., Jiang, H.L., 2003. Small envelope protein E of SARS: cloning, expression, purification, CD determination, and bioinformatics analysis. Acta Pharmacol. Sin. 24, 505–511.

Snijder, E.J., van Tol, H., Pedersen, K.W., Raamsman, M.J.B., de Vries, A.A.F., 1999. Identification of a novel structural protein of anteriviruses. J. Virol. 73, 6335–6345.

Sui, J., Li, W., Murakami, A., Tamin, A., Matthews, L.J., Wong, S.K., Moore, M.J., Tallarico, A.S., Olurinde, M., Choe, H., Anderson, L.J., Bellini, W.J., Farzan, M., Marasco, W.A., 2004. Potent neutralization of severe acute respiratory syndrome (SARS) coronavirus by a human mAb to S1 protein that blocks receptor association. Proc. Natl. Acad. Sci. U.S.A. 101, 2536–2541.

Suñé, C., Jiménez, G., Correa, I., Bullido, M.J., Gebauer, F., Smerdou, C., Enjuanes, L., 1990. Mechanisms of transmissible gastroenteritis coronavirus neutralization. Virology 177, 559–569.

Suñé, C., Smerdou, C., Antón, I.M., Abril, P., Plana, J., Enjuanes, L., 1991. A conserved coronavirus epitope, critical in virus neutralization, mimicked by internal-image monoclonal anti-idiotypic antibodies. J. Virol. 65, 6979–6984.

Thiel, V., Herold, J., Schelle, B., Siddell, S., 2001. Infectious RNA transcribed in vitro from a cDNA copy of the human coronavirus genome cloned in vaccinia virus. J. Gen. Virol. 82, 1273–1281.

Tooze, J., Tooze, S., Warren, G., 1984. Replication of coronavirus MHV-A59 in sac-cells: determination of the first site of budding of progeny virions. Eur. J. Cell Biol. 33, 281–294.

Tooze, J., Tooze, S.A., Fuller, S.D., 1987. Sorting of progeny coronavirus from condensed secretory proteins at the exit from the *trans*-golgi network of atT20 cells. J. Cell Biol. 105, 1215–1226.

van der Hoek, L., Pyrc, K., Jebbink, M.F., Vermeulen-Oost, W., Berkhout, R.J., Wolthers, K.C., Wertheim-van Dillen, P.M., Kaandorp, J., Spaargaren, J., Berkhout, B., 2004. Identification of a new human coronavirus. Nat. Med. 10, 368–373.

Van kuppeveld, F.J., Melchers, W.J., Kirkegaard, K., Doedens, J.R., 1997. Structure-function analysis of coxsackie B3 virus protein 2B. Virology 227, 111–118.

Vennema, H., Godeke, G.J., Rossen, J.W.A., Voorhout, W.F., Horzinek, M.C., Opstelten, D.J., Rottier, P.J.M., 1996. Nucleocapsid-independent assembly of coronavirus-like particles by co-expression of viral envelope protein genes. EMBO J. 15, 2020–2028.

Wilson, L., McKinlay, C., Gage, P., Ewart, G., 2004. SARS coronavirus E protein forms cation-selective ion channels. Virology 330, 322–331.

Wilson, L., Gage, P., Ewart, G., 2006. Hexamethylene amiloride blocks E protein ion channels and inhibits coronavirus replication. Virology 353, 290–306.

Yount, B., Curtis, K.M., Baric, R.S., 2000. Strategy for systematic assembly of large RNA and DNA genomes: the transmissible gastroenteritis virus model. J. Virol. 74, 10600–10611.

Yount, B., Curtis, K.M., Fritz, E.A., Hensley, L.E., Jahrling, P.B., Prentice, E., Denison, M.R., Geisbert, T.W., Baric, R.S., 2003. Reverse genetics with a full-length infectious cDNA of severe acute respiratory syndrome coronavirus. Proc. Natl. Acad. Sci. U.S.A. 100, 12995–13000.

Yu, X., Bi, W., Weiss, S.R., Leibowitz, J.L., 1994. Mouse hepatitis virus gene 5b protein is a new virion envelope protein. Virology 202, 1018–1023.

Zebedee, S.L., Lamb, R.A., 1988. Influenza A virus M2 protein: monoclonal antibody restriction of virus growth and detection of M2 in virions. J. Virol. 62, 2762–2772.